Simultaneous Measurement of Flowing Fluid Layer and Film Thickness of a Soap Bubble Using a UV−Visible Spectrophotometer

Tridib Kumar Sarma and Arun Chattopadhyay*

Department of Chemistry, Indian Institute of Technology, Guwahati, North Guwahati, Guwahati 781 039, India

Received April 23, 2001. In Final Form: July 31, 2001

In this Letter we report a method for observing Marangoni convection driven fluid flow, in various soap bubble systems, using a UV−visible spectrophotometer. We also report time-dependent simultaneous measurement of the thickness of the fluid layer and thickness of the bubble film. The measurement is based on earlier reports[1,2] of time-dependent monitoring of film thickness in a soap bubble by observing the interference maxima and minima occurring in the UV−visible region of wavelength. In the present case the interference maxima and minima due to the upward fluid flow appeared superimposed on those due to film thickness. Our observations suggest that the fluid layer thickness remains nearly constant for both vertical and horizontal bubbles even though the film thickness changes with time. The observed values of the fluid layer thickness are about 6.94 ± 0.15 μm for the vertical bubble and about 4.75 ± 0.09 μm for the horizontal bubble. Also, the intensity of the interference peaks due to Marangoni convection goes down as the film thickness reduces which indicates a possible decrease in refractive index of the fluid with time.

Introduction

The Marangoni effect (ME) is the flow of liquid driven by a surface tension gradient that can be created by a gradient of temperature or surfactant concentration. This effect is known to play a key role in interfacial transport of fluids, thinning of soap films,[3−6] and wetting and dewetting[7−13] behavior of thin liquid films with a wide range of applications that include lithography,[14] microscopic fluidic devices,[15,16] and spraying of insecticides, paints, and inks.[17] Owing to its technological application, the literature with both theoretical[18,19] and experimental[20,21] investigations under various conditions is vast and still growing. Spectroscopic[22−25] investigations in soap films have resulted in the understanding of time-dependent changes in film thickness, drainage of various components, microenvironments of the aqueous core of a black soap film, and the structure of thin films. On the other hand, there is a lack of data regarding the time-dependent thickness behavior of Marangoni convection driven fluid flow in soap films and bubbles and its relationship with the film thickness. We have sought to address the phenomena occurring in soap films by spectroscopic investigations of films in a soap bubble. In previous publications, one of us[1,2] reported the use of UV−visible and FTIR spectroscopic techniques to follow time-dependent changes in thickness and chemical composition of soap bubbles. Here we report UV−visible spectroscopic observation of a Marangoni flow driven upward movement of liquid in a soap bubble from a pool of soap solution. We also report the measurement of thickness of liquid flowing in single vertical and horizontal soap bubbles. A vertical bubble is a truncated spherical bubble sitting on top of an inverted beaker. The horizontal bubbles were blown from vertical soap films at the end of a horizontally aligned quartz tube. We also report an estimated thickness of the flowing liquid layer of about 6.94 ± 0.15 μm for a vertical bubble and 4.75 ± 0.09 μm for a horizontal bubble. The thickness in each case remained nearly constant throughout the observation period even though the thickness of the bubble film had changed considerably during that time. Our observations suggest that liquid from the reservoir flows upward along the bubble film due to the surface tension gradient created by stretching of a film to form soap bubble. The intensity of the interference maxima of absorbance due to the moving liquid layer diminished

* To whom correspondence may be addressed. E-mail: arun@iitg.ernet.in. Fax: +91-361-690762.

(1) Chattopadhyay, A. *Langmuir* **1999**, *15*, 7881.
(2) Chattopadhyay, A. *J. Chem. Educ.* **2000**, *77*, 1339.
(3) Exerowa, D. R.; Krugliakov, P. M. *Foams and Foam Films*: *Theory, Experiment, Application*; Studies in Interface Science; Elsevier: Amsterdam, 1998; Vol. 5.
(4) Prud'Homme, R. K., Khan, Saad A., Eds. *Foams*: *Theory, Measurements and Applications*; Surfactant Science Series; Mercel Dekker: New York, 1995; Vol. 57.
(5) Adamson, A. W.; Gast, A. P. *Physical Chemistry of Surfaces*, 6th ed.; John Wiley and Sons: New York, 1997.
(6) *Foams*: *Physics, Chemistry and Structure*; Wilson, A. J., Ed.; Springer-Verlag: Berlin, 1989.
(7) Troian, S. M.; Wu, X. L.; Safran, S. A. *Phys. Rev. Lett.* **1989**, *62* (13), 1496.
(8) Vanhook, S. J.; Schatz, M. F.; McCormick, W. D.; Swift, J. B.; Swinney, H. L. *Phys. Rev. Lett.* **1995**, *75* (24), 4397.
(9) Bestehorn, M. *Phys. Rev. Lett.* **1996**, *76* (1), 46.
(10) de Ruijter, M. J.; Blake, T. D.; De Connick, J. *Langmuir* **1999**, *15*, 7836.
(11) Semal, S.; Voue, M.; De Connick, J. *Langmuir* **1999**, *15*, 7848.
(12) Reiter, G.; Khanna, R. *Langmuir* **2000**, *16*, 6351.
(13) Bergeron, V.; Bonn, D.; Martin, J. Y.; Vovelle, L. *Nature* **2000**, *405*, 772.
(14) Xia, Y.; Whitesides, G. M. *Angew. Chem., Int. Ed. Engl.* **1998**, *37*, 550.
(15) Kataoka, D. E.; Troian, S. M. *Nature* **1999**, *402*, 794.
(16) Delamarche, E.; Benard, A.; Schmidt, H.; Michel, B.; Biebuyck, H. *Science* **1997**, *276*, 779.
(17) Carré, A.; Gastel, J. C.; Shanahan, M. E. R. *Nature* **1996**, *379*, 432.
(18) Golovin, A. A.; Nepomnyashchy, A. A.; Pismen, L. M. *J. Fluid. Mech.* **1997**, *341*, 317.
(19) Denniston, C.; Yeomans, J. M. *Phys. Chem. Chem. Phys.* **1999**, *1*, 2157.
(20) Yaminsky, V. V.; Thuresson, K.; Ninham, B. W. *Langmuir* **1999**, *15*, 3683.
(21) Yerushalmi − Rozen, R.; Kerle, T.; Klien, J. *Science* **1999**, *285*, 1254.
(22) Umemura, J.; Matsumoto, M., Kawai, T.; Takenaka, T. *Can. J. Chem.* **1985**, *63* (7), 1713.
(23) Cohen, R.; Exerowa, D.; Kolarov, T.; Yamanaka, T.; Tano, T. *Langmuir* **1997**, *13*, 3172.
(24) Du, X.; Liang, Y. *Phys. Chem. Chem. Phys*, **2000**, *2*, 137.
(25) Bélorgey, O.; Benattar, J. J. *Phys. Rev. Lett.* **1991**, *66*, 313.

10.1021/la010594z CCC: $20.00
Published on Web 09/12/2001

gradually with the thinning of the bubble film. The flow was not observed after some time, although the film thickness was considerably higher than the final low thickness. The thickness of the fluid flowing upward was observed to be much larger than the film thickness and was independent of the film thickness.

Partial reflections of a beam of light from the surfaces of a thin, semitransparent film cause interference in the light. The interference fringes become visually observable when the film thickness is of the order of a wavelength of visible light. Thus if a soap film is kept inside the sample compartment of a UV-visible spectrophotometer and the wavelength of light is scanned, a set of maxima and minima of absorbance occurring at different wavelengths is observed. The number of such maxima and minima and the separation between two consecutive maxima or minima depend on the thickness of the bubble film and thus can be used to monitor the film thickness. The following equations are used to calculate the thickness of the soap films from the positions of maxima and minima of absorbance

$$\nu = \left[\frac{n(\lambda_1)}{\lambda_1} - \frac{n(\lambda_2)}{\lambda_2}\right]/N_{\text{cyc}} \quad (1)$$

$$d = (2\nu)^{-1} \quad (2)$$

Here $n(\lambda_1)$ and $n(\lambda_2)$ are the refractive indices of the film at wavelengths λ_1 and λ_2. N_{cyc} is the number of cycles in the interference fringes, and d is the thickness of the film. In a bubble generally the light beam travels through two such films. Considering the drainage to be symmetrical around the vertical axis of the bubble, it may be assumed that the thicknesses of both the films are same at any point of time. The interference pattern arising out of light passing through two such films would be same as that of a single film. Thus the thickness obtained by applying eqs 1 and 2, to the experimentally observed absorption maxima and minima would be the thickness of one such film. The above equations can also be used to measure the thickness of a ME-driven fluid flow in a stretched soap film as described below. For our results we have not taken into account the error due to the curvature of the bubble films while using the above equations, as the measurements are quite slow and the error due to variations in thickness during the measurement is larger than that due to the assumption (See Appendix).

Marangoni effect driven fluid flow also resulted in the appearance of interference absorption maxima and minima similar to those due to film thickness except for the fact that the wavelength separation between two maxima or minima arising out of ME is much smaller than those due to film thickness. The UV−vis absorption spectrum of a bubble consisted of a set of narrowly spaced, weaker absorption maxima and minima superimposed on widely spaced and stronger absorption maxima and minima. This makes it possible to simultaneously measure the thickness of a soap film and the thickness of Marangoni flow driven fluid layer.

Experimental Section

Soap bubbles of about 19 mm diameter were made from a solution containing a mixture of 0.2 g (0.07 M) of sodium dodecyl sulfate (SDS) and 0.02 g (0.01 M) of 1-dodecanol in 10 mL of Millipore-filtered water. Horizontal films and bubbles were made from the horizontal end of a T-shaped quartz tube that was kept hanging from the lid of a 250 mL beaker (Figures 1, 3, and 4). Vertical bubbles were made from a solution poured over an inverted 10 mL beaker kept inside the 250 mL beaker (Figure 2). For the horizontal bubble a film was first formed at one horizontal end of the tube by dipping into the soap solution, while the other end of the tube was closed with a sapphire window. The third opening of the tube was closed with a rubber stopper and used for air blowing or injecting solution. The film was then blown into a bubble. About 0.5 mL of the soap solution was then injected into the tube such that a drop of the solution remained hanging at the bottom of the bubble. To increase the stability of the bubbles, the humidity of the chamber was increased by placing a piece of ordinary filter paper soaked with water inside the beaker. Optical measurements of individual bubbles were performed by putting the larger beaker inside the sample compartment of a Hitachi U 2001 UV−visible spectrophotometer. For calculation of film thickness as well as flowing fluid layer thickness, we have used a value of 1.333 as the refractive index

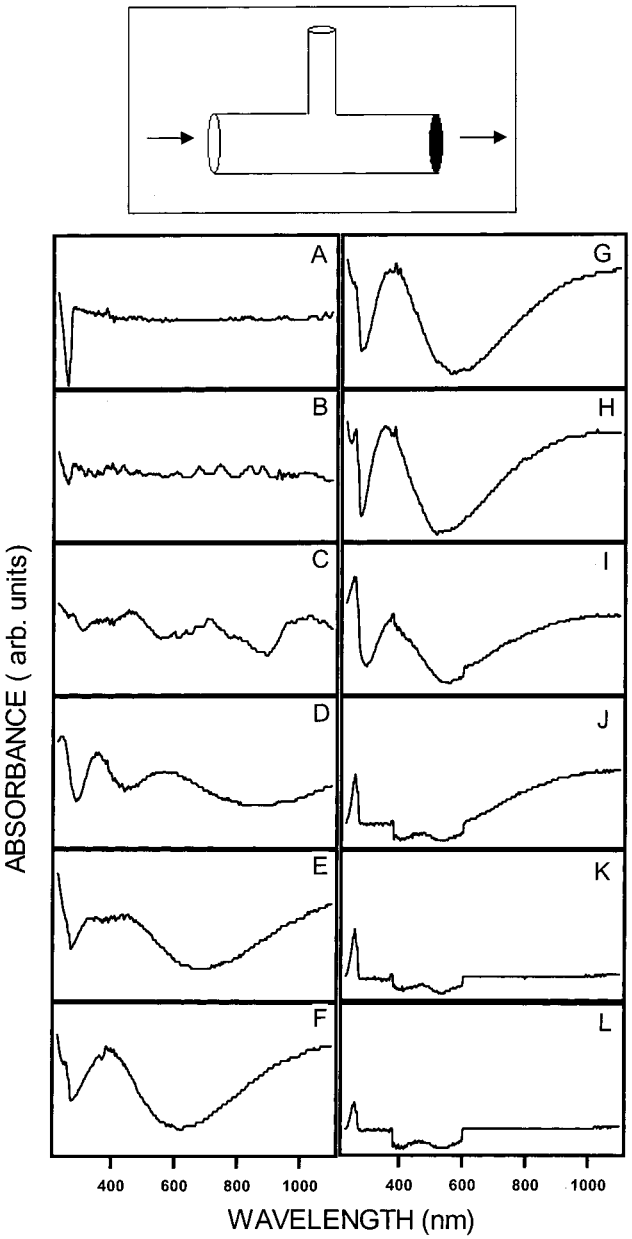

Figure 1. (top) Schematic representation of the experimental setup containing a vertical soap film. (below) Time-dependent UV−vis spectra of the vertical film: (A) 0−2 min; (B) 5−6 min, d_2 = 624 nm; (C) 7−8 min, d_2 = 472 nm; (D) 9−10 min, d_2 = 396 nm; (E) 11−12 min, d_2 = 270 nm; (F) 13−14 min, d_2 = 254 nm; (G) 17−18 min, d_2 = 242 nm; (H) 29−30 min, d_2 = 240 nm; (I) 88−89 min, d_2 = 228 nm; (J) 90−91 min; (K) 92−93 min; (L) background spectrum after bursting the film after 95 min from the time of formation. d_2 = estimated thickness of the vertical film.

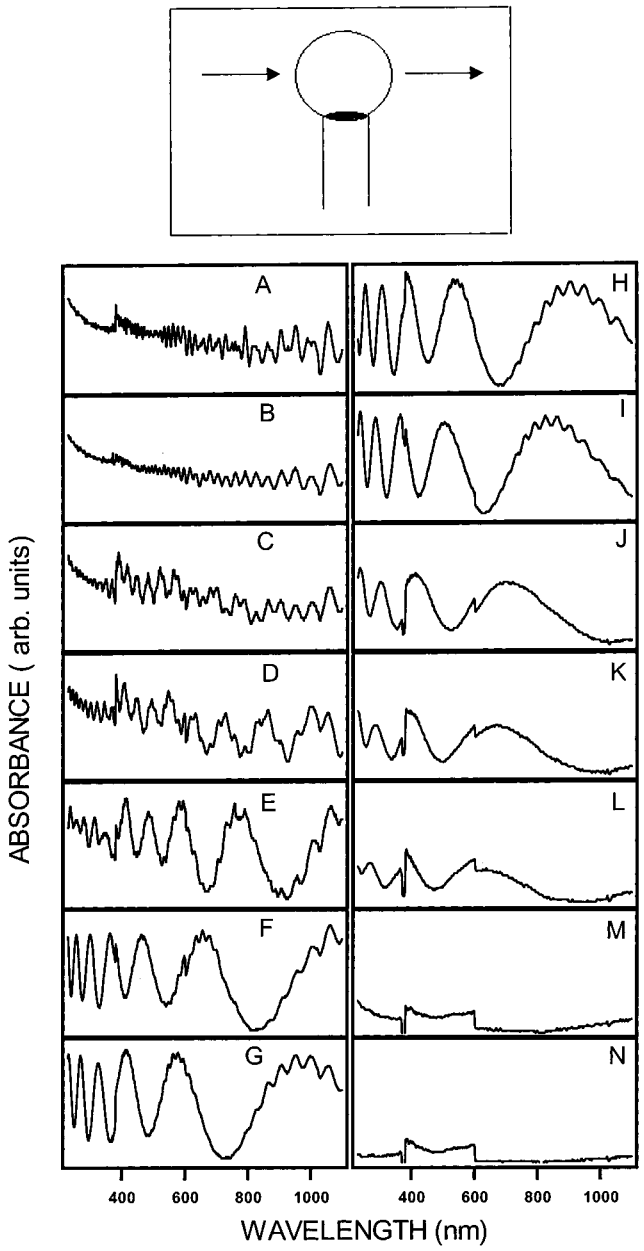

Figure 2. (top) Schematic representation of the experimental setup containing a vertical soap bubble. (below) UV−vis absorption spectra of the vertical bubble: (A) 0−2 min, d_1 = 7.16 μm; (B) 6−8 min, d_1 = 7.11 μm; (C) 16−18 min, d_1 = 7.04 μm; (D) 19−20 min, d_1 = 6.9 μm, d_2 = 1781 nm; (E) 21−22 min, d_1 = 6.81 μm, d_2 = 995 nm,; (F) 28−30 min, d_1 = 6.82 μm, d_2 = 647 nm; (G) 34−36 min, d_1 = 6.85 μm, d_2 = 579 μm; (H) 40−41 min, d_1 = 6.82 μm, d_2 = 536 nm; (I) 50−51 min, d_1 = 6.87 μm, d_2 = 482 nm; (J) 62−63 min, d_2 = 408 nm; (K) 64−65 min, d_2 = 378 nm; (L) 66−67 min, d_2 = 364 nm; (M) 68−69 min; (N) background spectra after bursting the vertical bubble after 70 min of formation. d_1 = estimated thickness of the water peaks. d_2 = estimated thickness of the bubble film.

and have assumed that it is independent of film thickness or fluid layer thickness (See Appendix). The experiments were performed typically in the temperature range of 21−25 °C.

Results and Discussion

At first, we present the results obtained from a single vertical soap film that was placed on one end of a horizontally aligned quartz tube. The other end of the tube was kept open, thereby removing the possibility of having any curvature of the soap film. The UV−vis absorption spectra of a stable film are shown in Figure 1. As clear from the set of spectra the thickness decay was gradual and slow. There were no observable interference peaks due to ME fluid flow. The peaks due to thickness of the film started appearing in about 7 min from the time of formation as shown in Figure 1D. The thickness changed from 472 nm at 7−8 min to about 228 nm at about 88 min from the time of the formation of the film. The film then became very thin, and interference fringes no longer appeared. At this thickness, the film remained stable for hours. The above results are generally observed for a very stable film whose thickness changes slowly. Throughout the observation period the interference fringes due to ME flow were not observed.

Figure 2 shows a collection of typical time-dependent UV−vis absorption spectra of a vertical bubble. The light beam passed through two films of the bubble. The interference fringes started appearing from the time of the formation of the bubble. We believe that these fringes occurred due to the Marangoni effect as they had been observed for a long time with nearly constant thickness of the fluid layer and such fringes did not appear in the case of the vertical film (Figure 1). Also, the interference fringes due to ME fluid flow could be seen appearing superimposed on the interference fringes occurring due to thickness changes of the film (Figure 2D−I). The thickness of the ME fluid layer remained nearly constant with a value varying between 7.16 and 6.81 μm. The fluid flow could also be observed when an ordinary diode laser pointer beam (red) was passed through the bubble and then defocused with a 10 cm focal length lens and projected onto a wall. A fountain of fluid could be seen moving up in the beginning, and with time, drops of fluid were observed moving up along the bubble. The fluid flow was not observed when the bubble film had become thinner and colorless. The results shown in Figure 2D−I require particular attention since the ME fluid layer thickness remained nearly constant with values between 6.90 and 6.81 μm even though the thickness of the film had decreased from 1781 to 482 nm. This might be due to two parallel processes occurring simultaneously in the bubble film. While the thickness of the film decreased due to drainage of the components, the restoring fluid moved upward. This could be observed until the thickness of the film was about 482 nm after which the film thickness continued to reduce due to drainage whereas ME driven fluid movement was not observed. It is possible that the upward movement of fluid continues, until the film thickness becomes very thin and constant, but could not be observed for a longer time here due to weak signal intensity, whereas the interference peaks due to film thickness remain stronger for a longer period of time. The gradual decrease in intensity of the interference peaks with time due to ME fluid flow is evident in Figure 2B−I.

The time-dependent absorption spectra due to ME fluid convection and thickness changes of the bubble films of two horizontal bubbles, one probed along the axis of the bubble and the other perpendicular to it, are shown in Figures 3 and 4, respectively. These measurements correspond to a film stretched into a bubble. A drop of solution was kept hanging at the bottom of the bubble (added after its formation) for improved signal of the ME fluid flow. Like the vertical bubble, for both the measurements, the first few absorption spectra consisted of maxima and minima due to ME fluid movement only. The fluid layer thickness values are 4.62, 2.90, and 2.84 μm for spectra in parts A, B, and C of Figure 3, respectively, and 4.82, 4.89, 4.80, and 4.76 μm for spectra in panels A−D of Figure 4, respectively. These values are obtained from

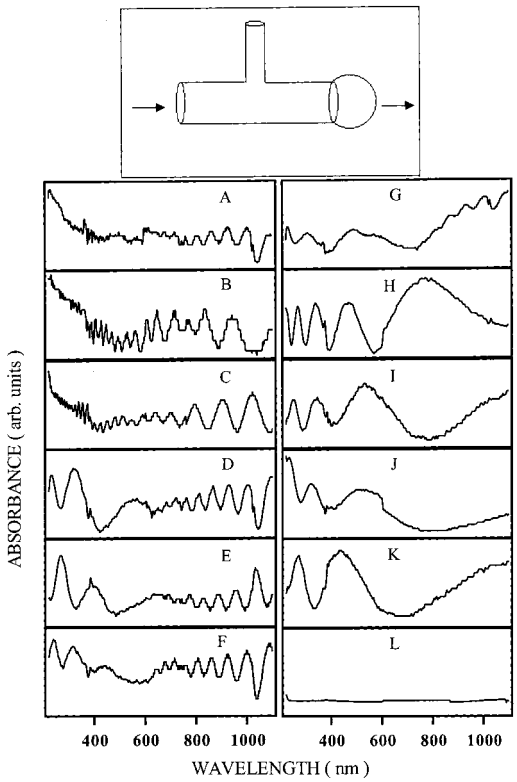

Figure 3. (top) Schematic representation of the experimental setup containing the horizontal bubble probed axially. (below) Time-dependent UV−vis absorption spectra of the axially probed horizontal bubble: (A) 0−2 min, $d_1 = 4.62\ \mu$m; (B) 3−4 min, $d_1 = 2.90\ \mu$m; (C) 5−6 min, $d_1 = 2.84\ \mu$m; (D) 7−8 min, $d_1 = 4.66\ \mu$m, $d_2 = 276$ nm; (E) 9−10 min, $d_1 = 4.70\ \mu$m, $d_2 = 320$ nm; (F) 11−12 min, $d_1 = 4.68\ \mu$m, $d_2 = 378$ nm; (G) 13−14 min, $d_1 = 4.70\ \mu$m, $d_2 = 358$ nm; (H) 15−16 min, $d_2 = 480$ nm; (I) 17−18 min, $d_2 = 340$ nm; (J) 19−20 min, $d_2 = 310$ nm; (K) 21−22 min, $d_2 = 240$ nm; (L) 23−24 min. d_1 = estimated thickness of the fluid layer occurring due to Marangoni effect. d_2 = estimated thickness of the bubble film.

the observed spectra during the first 6 min of measurement (8 min for the perpendicular to the axis probe case) after the bubble formation. The film thickness peaks started appearing in about 7 min as shown in Figure 3 (9 min as in Figure 4). Hereafter the absorption maxima originating from ME fluid flow were weak, and only rough estimates could be made about the thickness. The estimated thickness values of the ME-driven flowing fluid are about 4.66, 4.70, 4.68, and 4.70 μm (parts D−G of Figure 3, respectively) while the film thickness went up from 276 to 358 nm. It is interesting to note here that for the axially probed horizontal bubble, the film thickness had already gone down to about 276 nm in about 7 min from the formation of the bubble. The thickness then went up to about 378 nm in about 12 min and then again went down. Similar results were obtained for the bubble probed sideways as shown in Figure 4. Other observations that require particular attention are the values of thickness of the ME fluid layer in parts B and C of Figure 3, 2.90 and 2.84 μm, respectively. These values are very different from the average value of $4.75 \pm 0.09\ \mu$m observed for the horizontal films probed both axially and sideways.

Conclusion

In this Letter, we have reported the observation of a Marangoni convection driven upward movement of fluid up along single vertical and horizontal soap bubble systems. We also have reported the thickness of such fluid

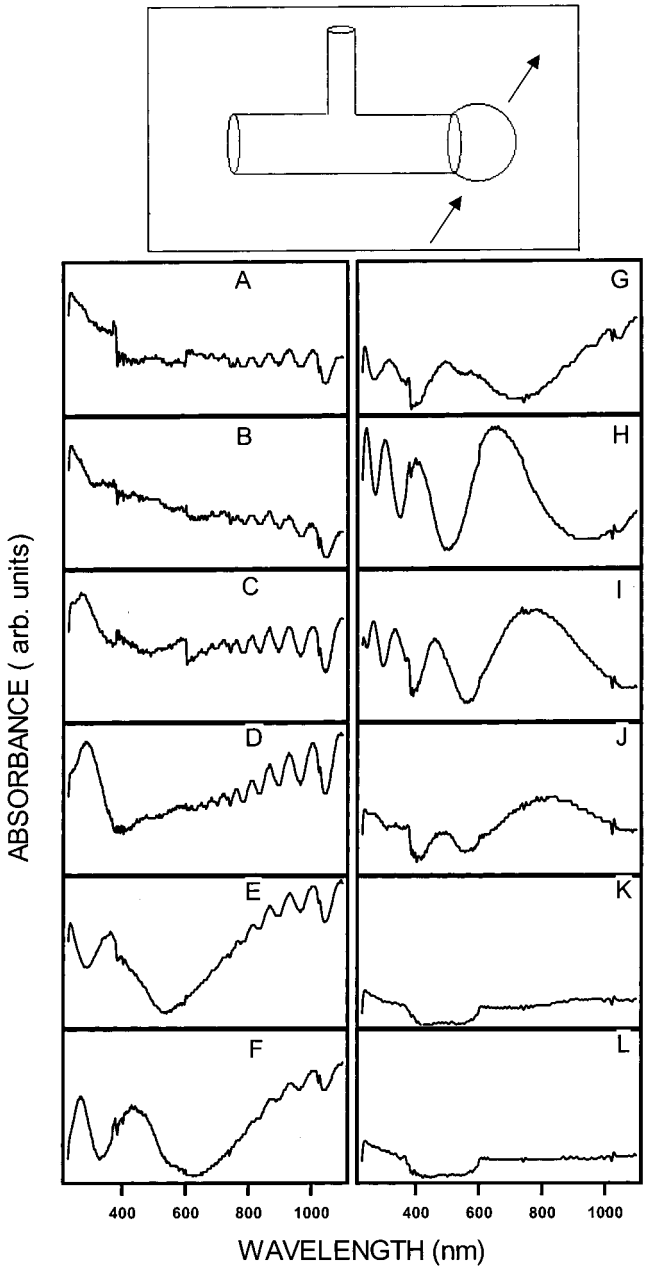

Figure 4. (top) Schematic representation of the experimental setup containing horizontal bubble probed sideway. (below) Time-dependent UV−vis absorption spectra of the above horizontal bubble: (A) 0−2 min, $d_1 = 4.82\ \mu$m; (B) 3−4 min, $d_1 = 4.89\ \mu$m; (C) 5−6 min, $d_1 = 4.80\ \mu$m; (D) 7−8 min, $d_1 = 4.76\ \mu$m; (E) 9−10 min, $d_1 = 4.65\ \mu$m, $d_2 = 270$ nm; (F) 11−12 min, $d_1 = 4.68\ \mu$m, $d_2 = 364$ nm; (G) 13−14 min, $d_1 = 4.65\ \mu$m, $d_2 = 386\ \mu$m; (H) 15−16 min, $d_2 = 524$ nm; (I) 17−18 min, $d_2 = 341$ nm; (J) 19−20 min, $d_2 = 244$ nm; (K) 21−22 min; (L) 23−24 min, background spectrum after bursting the bubble. d_1 = estimated thickness of the fluid layer occurring due to Marangoni effect. d_2 = estimated thickness of the bubble film.

layers in various bubble systems as they evolve with time. For a vertical bubble the fluid layer thickness was about $6.94 \pm 0.15\ \mu$m and the thickness remained nearly constant even though the film thickness went down with time. Similarly, for a horizontal bubble this thickness was about $4.75 \pm 0.09\ \mu$m and remained nearly constant throughout the observation period. Our observations suggest that ME effect driven fluid flow runs in parallel with the film drainage but in an opposite direction. The signal intensity due to Marangoni fluid flow becomes weaker as the film

thickness gets smaller. Among other factors, like the film thickness, the decrease in refractive index[26] of the fluid layer may contribute to the decrease in the transmitted light intensity.

Acknowledgment. This project was funded by CSIR, New Delhi (Grant No. 01(1578)/99/EMR-II). We thank Dr. P. Senthilkumaran for helpful discussions.

Appendix

When a light beam of parallel rays impinges on a spherical soap bubble (Figure 5) and where θ is the angle of incidence, R is the radius of curvature of the sphere, d is the thickness of spherical film, $n(\lambda)$ is the refractive index of the film at wavelength λ, H is the height of the incident light beam from the center, and N is the number of cycles in the interference fringes, then

$$\theta = 90° - \cos^{-1}(H/R) \tag{A1}$$

For constructive interference, using the equation of thin parallel films

$$\frac{2n(\lambda_2)d\cos\theta}{m+1} = \lambda_2 \tag{A2}$$

and

$$\frac{2n(\lambda_1)d\cos\theta}{m+N+1} = \lambda_1 \tag{A3}$$

Therefore

$$d = \frac{N}{2\cos\theta}\left[\frac{n(\lambda_1)}{\lambda_1} - \frac{n(\lambda_2)}{\lambda_2}\right]^{-1} \tag{A4}$$

In our experimental apparatus, maximum height of the light beam was about 4 mm (the width of the beam was about 1 mm) and the radius of curvature of the film was about 9.5 mm, and hence maximum deviation from normal incidence would be about 24.9° corresponding to an error in measurement of about 10% (if the equation corresponding to normal incidence is used instead, i.e., eq 2 instead of eq A4). Considering the variation of angle of incidence at different height of the beam, if we take an average value of H to be 2 mm (angle of incidence 12.2°), then the average deviation turns out to be 2.3%. This is nearly equal to the error limit of the calculated results of the experiment data.

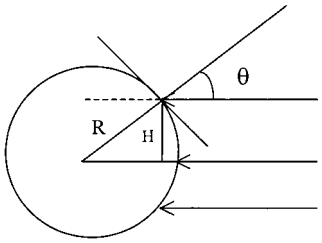

Figure 5. Drawing of a light beam of parallel rays impinging on a spherical soap bubble.

Table 1. Film Thickness Calculations Obtained by Using Equation 4A at Various Wavelength Ranges and an Angle of Incidence of 12.2°

wavelength range (nm)	film thickness (nm)	wavelength range (nm)	fluid layer thickness (μm)
277−332	1760		
467−585	1790	686−773	6.99
776−926	1846	974−1090	6.92

For example, consider the spectra in parts D and E of Figure 2 separated by an average measurement time of 2 min. If eq 2 is used, the average thickness of film is calculated to be 1767 nm and that of fluid layer is 6.76 μm for spectrum D in Figure 2 while those values are found to be 1808 nm and 6.92 μm if eq A4 is used instead. The corresponding calculations for spectrum E in Figure 2 result in a film thickness value of 996 nm and fluid layer thickness value of 6.76 μm if eq 2 is used and 1016 nm and 6.91 μm if eq A4 is used. Also, for spectrum D of Figure 2, results of calculations using eq A4 at various wavelength ranges and for an angle of incidence of 12.2° are shown in Table 1.

Thus while using eq 2 or A4, we obtain values close to each other for each graph and the thickness value changes dramatically in 2 min of measurement time. Also, the variation of thickness during a single complete scan of wavelength ranges is significant (calculations from Figure 2D). Hence the use of eq 2 may be sufficient for the above calculations. In all the calculations above, the values of refractive indices were taken from ref 27.

LA010594Z

(26) Huibers, P. D. T.; Shah, D. O. *Langmuir* **1997**, *13*, 5995.

(27) Huibers, P. D. T. *Appl. Opt.* **1997**, *36*, 3785.